Supplementary figure 1

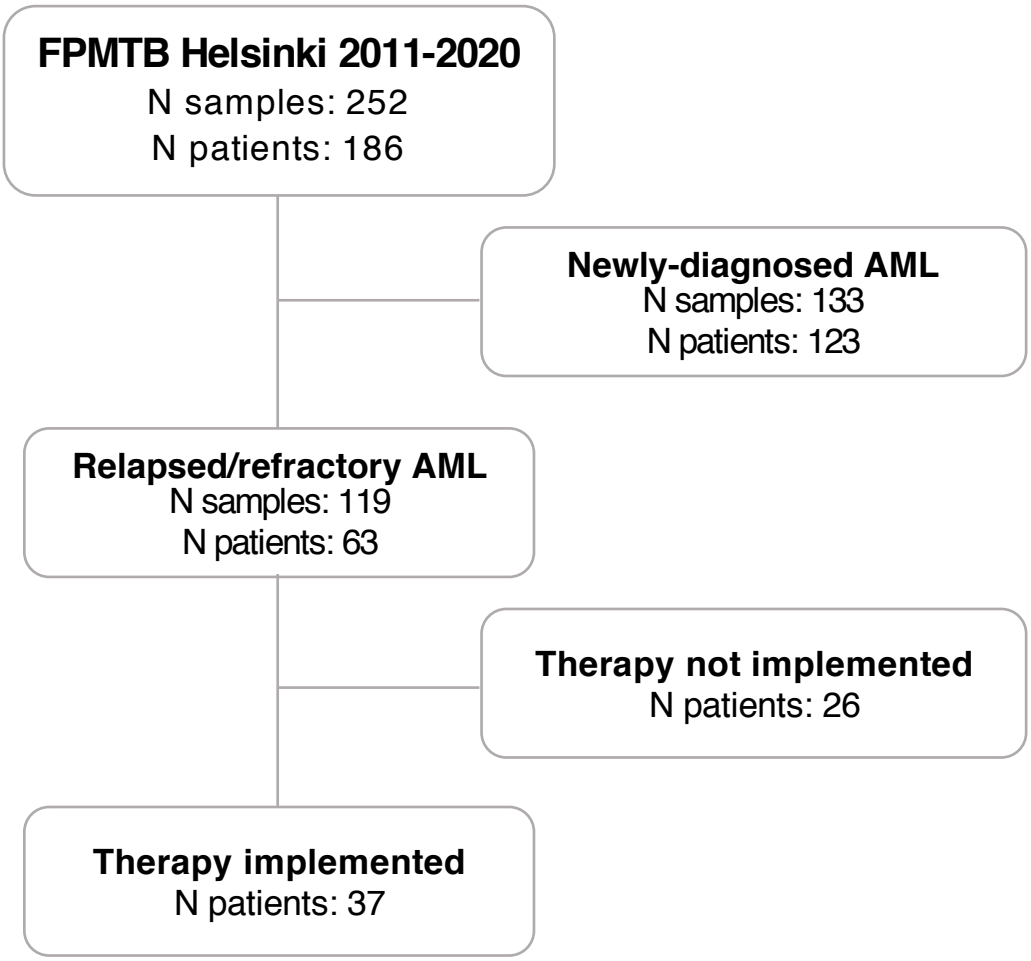

Supplementary Figure 1. Consort diagram. CONSORT diagram of patient and sample flow discussed at the Functional Precision Medicine Tumor Board (FPMTB) meetings of the Helsinki University Hospital Cancer Center. Newly diagnosed patients were treated with standard of care or in a clinical study and their molecular and functional profiling data were used for correlative analyses. For the relapsed or refractory cohort, patients fulfilling the inclusion criteria (see Supplementary Table 1) were treated according to FPMTB recommendations as compassionate use and as series of consecutive patients. Note that some patients had samples both at the time of diagnosis and at relapse(s), see Supplemental Table 3 for details.

Supplementary figure 2

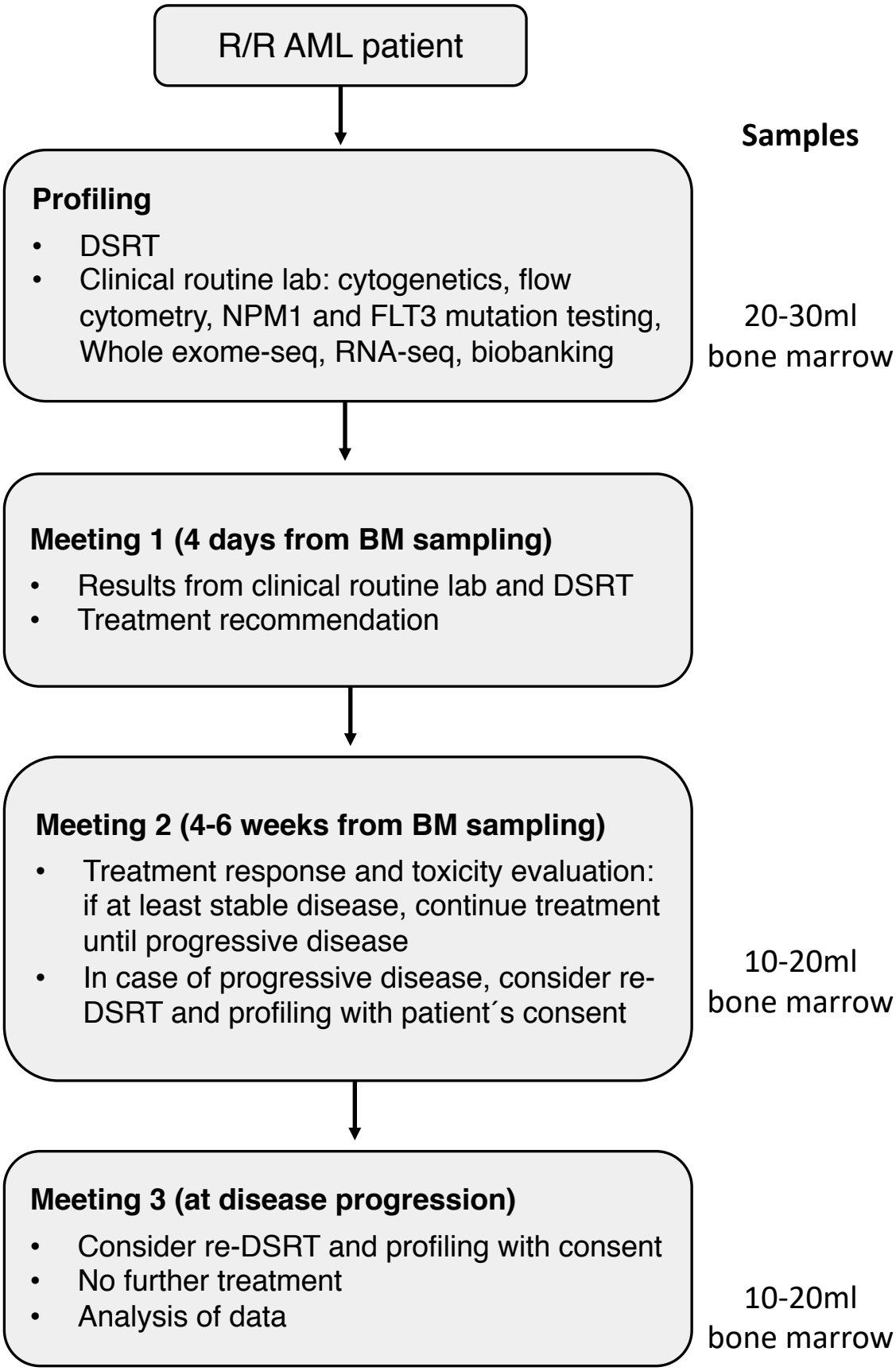

Supplementary Figure 2. The FPMTB workflow. The functional precision medicine tumor board workflow, including patient bone marrow sampling timepoints.

Supplemetary figure 3

a.

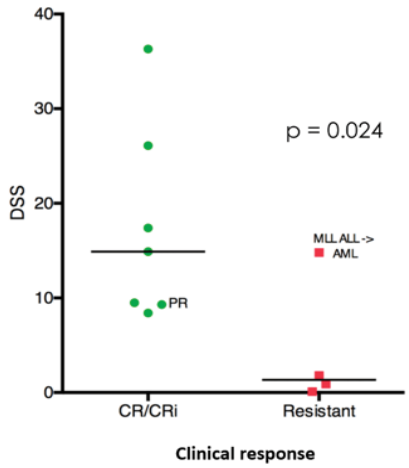

b.

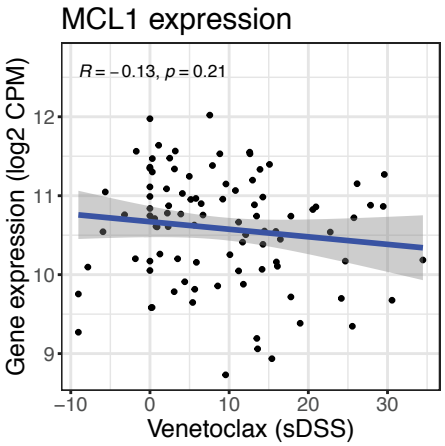

c.

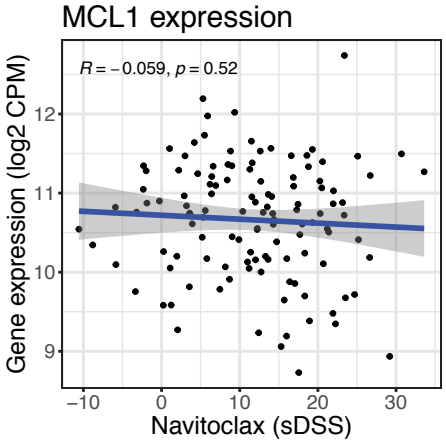

d.

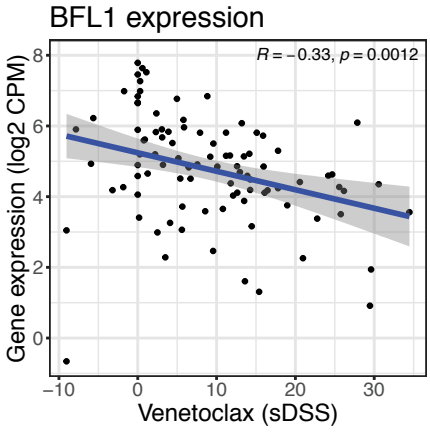

e.

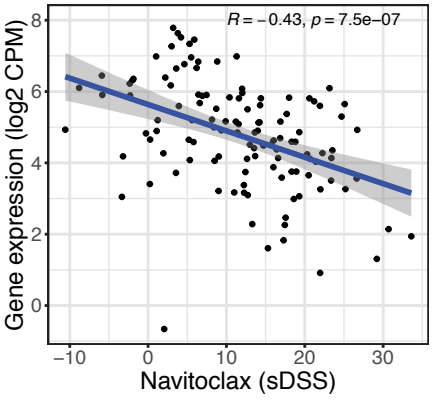

Supplementary Figure 3. Tumor board criteria. a, *Ex vivo* drug responses and corresponding clinical outcome of the venetoclax therapy in 11 AML patients. **b-c,** Correlation of RNA-seq based expression of *MCL1* gene with *ex vivo* response to venetoclax and navitoclax. **d-e,** Correlation of RNA-seq based expression of *BFL1 (BCL2A1)* gene with *ex vivo* response to venetoclax and navitoclax.

Supplementary figure 4

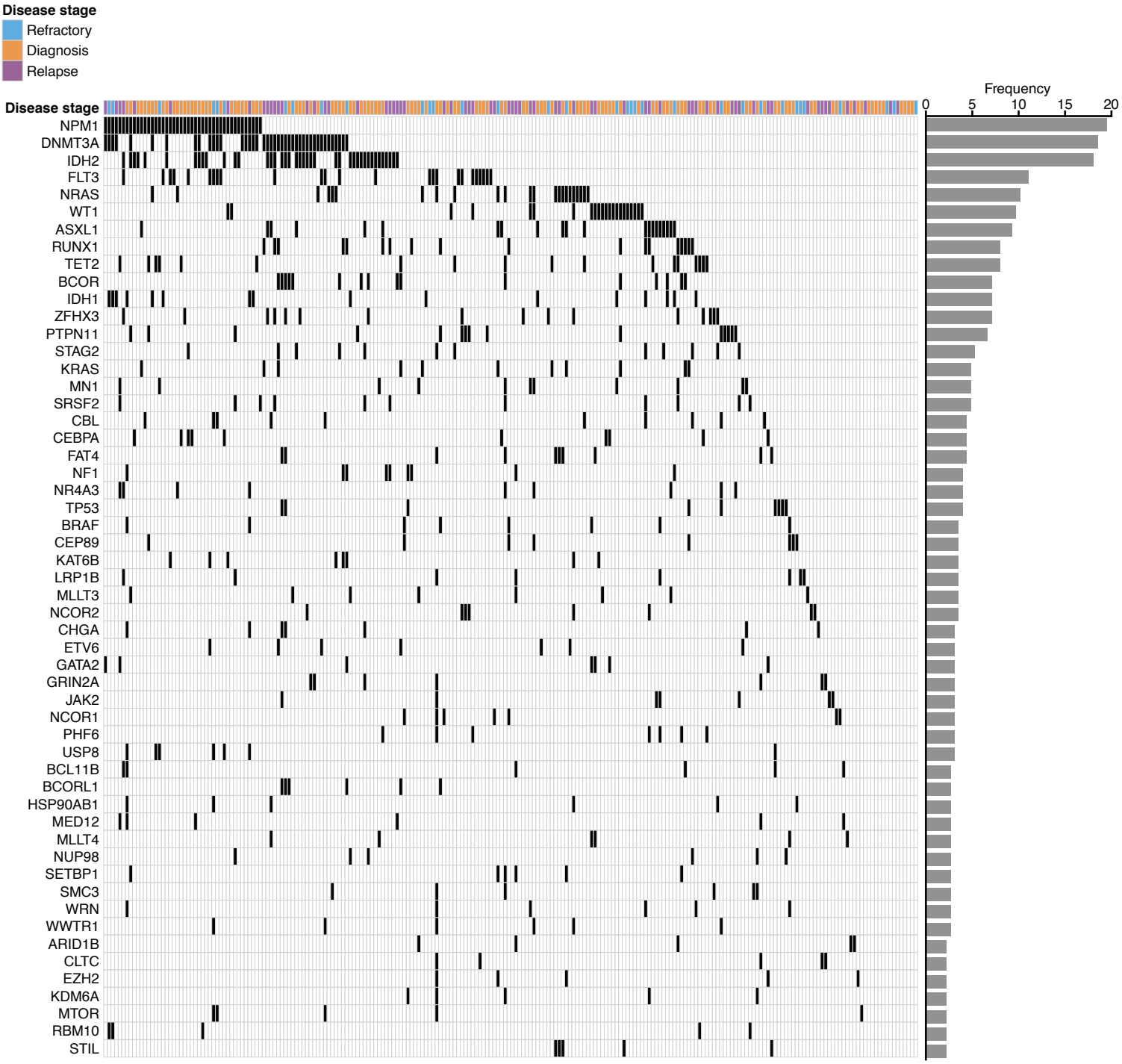

Supplementary Figure 4. Mutational landscape. The somatic mutation data for 226 AML patient samples arranged as per the recurrence of mutated genes. Somatic mutations were considered with P values < 0.05 and the highest mutation frequency was considered if the gene was mutated more than once in the same sample. The data is shown for 57 cancer or AML related genes if mutation found in at least five samples.

Supplementary figure 5

a

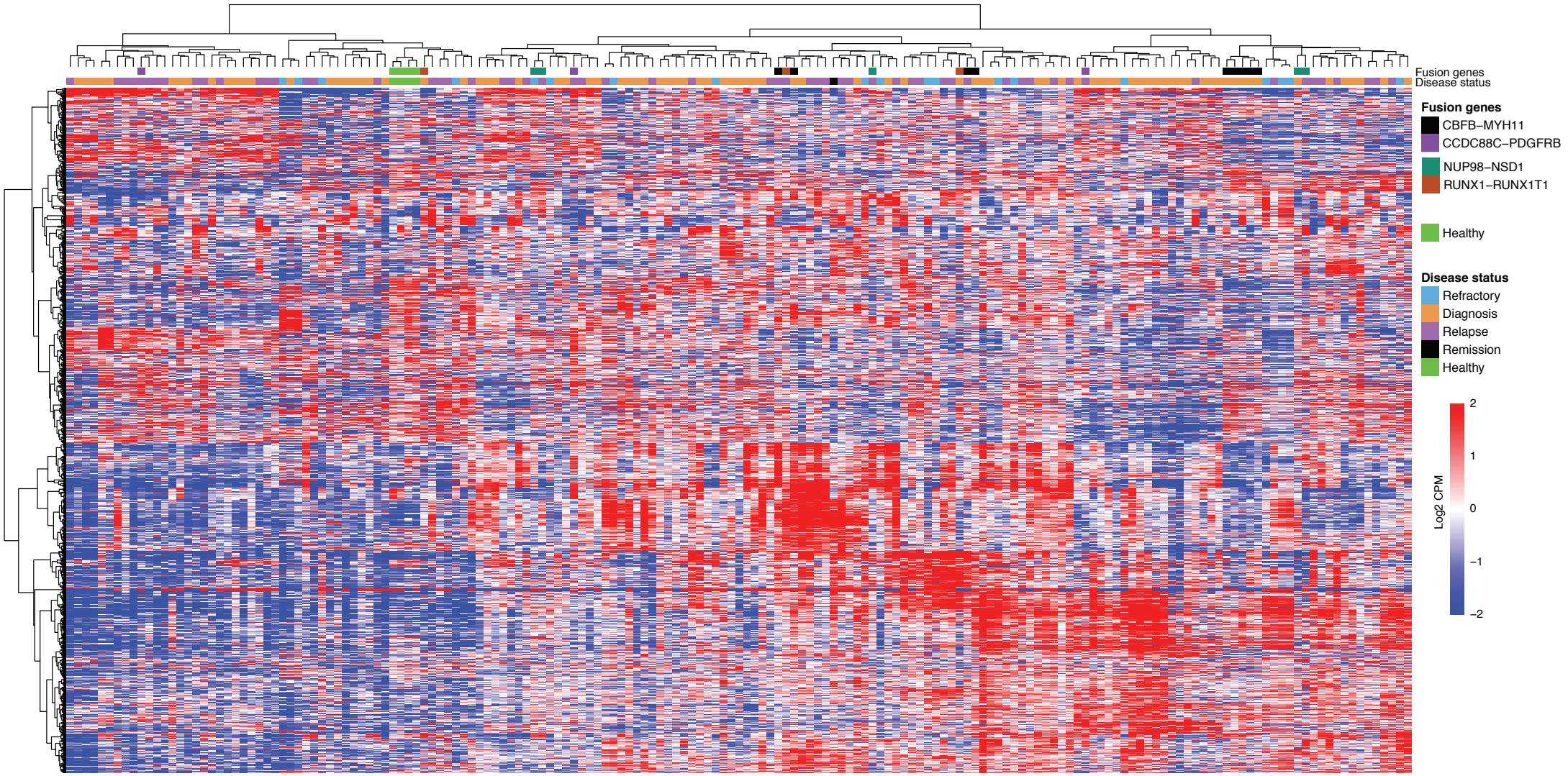

b

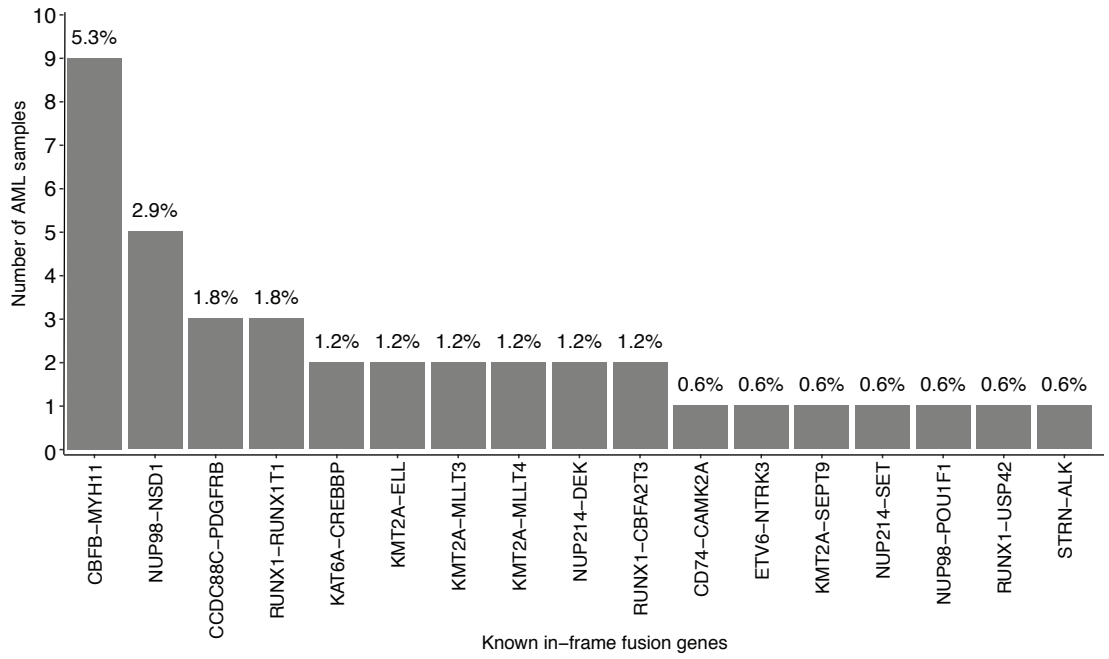
Number of AML samples
10
9
8
7
6
5
4
3
2
1
0
5.3%
2.9%
1.8%
1.8%
1.2%
1.2%
1.2%
1.2%
1.2%
1.2%
0.6%
0.6%
0.6%
0.6%
0.6%
0.6%
0.6%
CBFB–MYH11
NUP98–NSD1
CCDC88C–PDGFRB
RUNX1–RUNX1T1
KAT6A–CREBBP
KMT2A–ELL
KMT2A–MLLT3
KMT2A–MLLT4
NUP214–DEK
RUNX1–CBFA2T3
CD74–CAMK2A
ETV6–NTRK3
KMT2A–SEPT9
NUP214–SET
NUP98–POU1F1
RUNX1–USP42
STRN–ALK
Known in–frame fusion genes

c

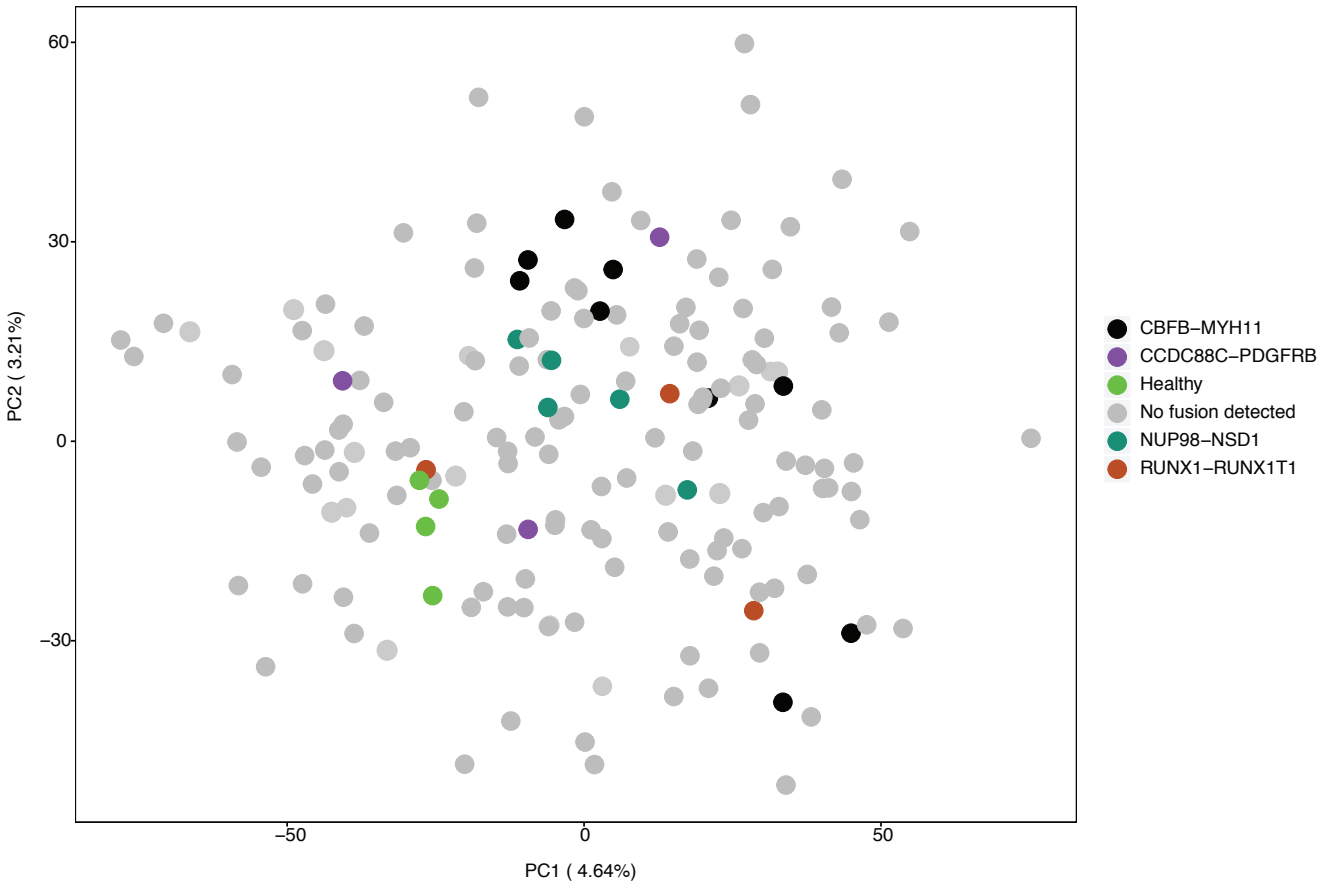
60
30
0
−30
PC2 (3.21%)
−50
0
50
PC1 (4.64%)
CBFB–MYH11
CCDC88C–PDGFRB
Healthy
No fusion detected
NUP98–NSD1
RUNX1–RUNX1T1

Supplementary Figure 5. Gene expression patterns and fusion gene frequencies. a, Hierarchical clustering of 163 AML patients and 4 healthy control samples (Euclidean distance) and 20,000 protein-coding genes (correlation distance) using complete linkage. The fusion gene annotation indicating gene expression profile dependent on type of fusion. **b,** Frequency of fusion genes in 163 AML patient samples. **c,** PCA plot illustrating impact of fusion genes on grouping of samples based on gene expression profiles.

Supplementary figure 6

a

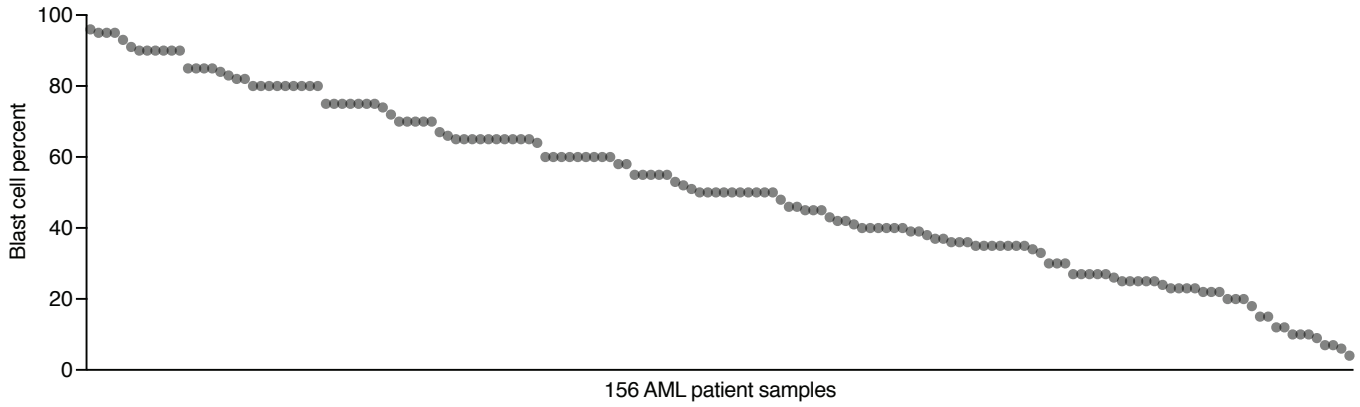

b

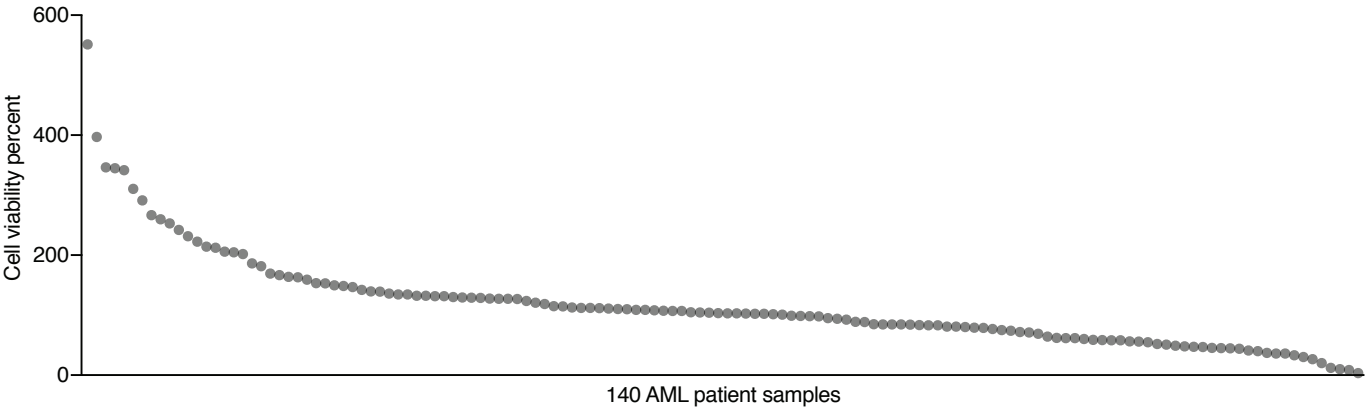

Supplementary Figure 6. Correlation of drug responses with blast cells and cell viability. a, Distribution of blast cell percent across 156 AML patient samples. **b,** Distribution of cell viability percent for 140 AML patient samples. The cell viability percent is a measurement of cell survival ratio between 0 and 72 hours in absence of drug.

Supplementary figure 7

a

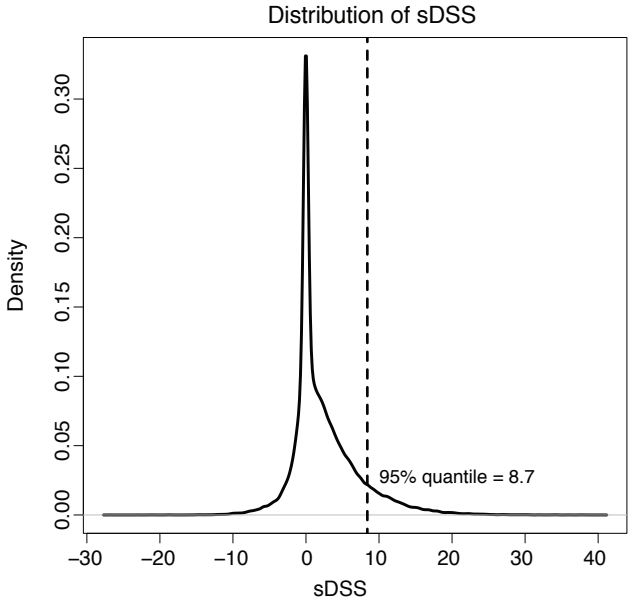

b

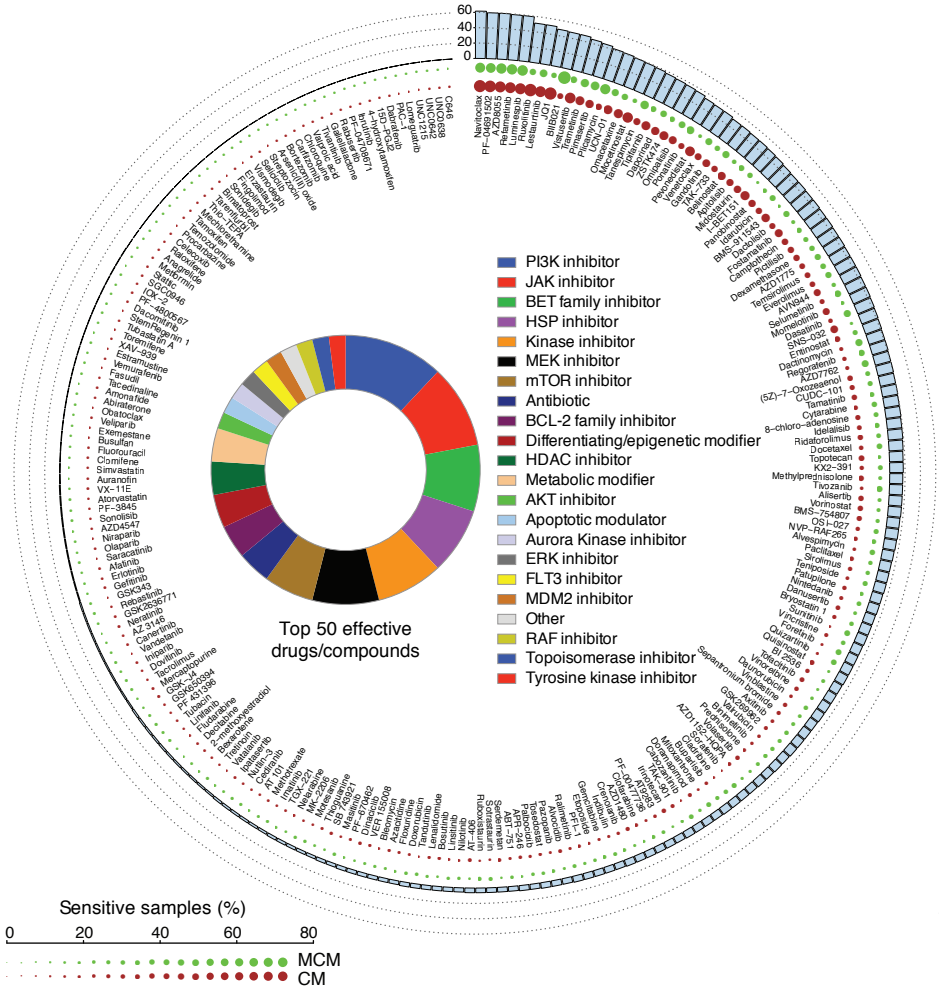

c

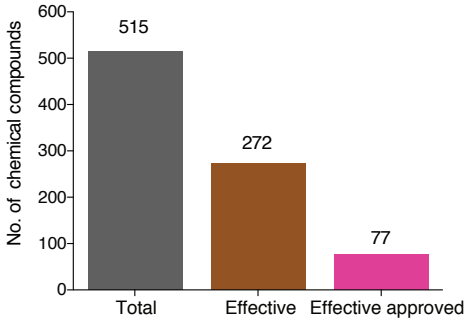

d

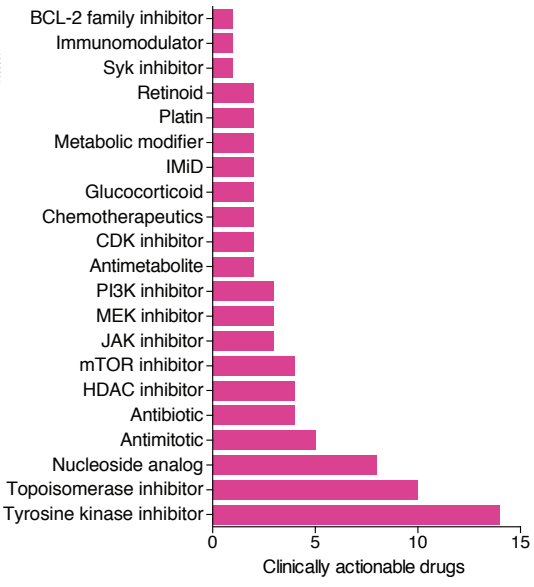

Supplementary Figure 7. Drug response overview. a, Distribution of sDSS from overall drug testing data where 95% quantile indicating 8.7 sDSS to define the efficacy of drugs. **b,** In the circular plot created using the circlize R-package, the blue bars depict a percentage of 164 AML patient samples sensitive for 238 effective drugs with data available in both sample sets. Similarly, the dot size represents the percentages of samples sensitive to respective drugs tested in MCM (green) or CM (brown) medium. **c,** Number of total drugs used for drug testing, effective drugs (at least 3 samples sensitive to a respective drug) and approved drugs deconvoluted from *ex vivo* drug testing in AML patients. **d,** Sub-classes of approved targeted drugs showing high efficacies across all samples and representing actionable AML therapeutic drugs.

Supplementary figure 8

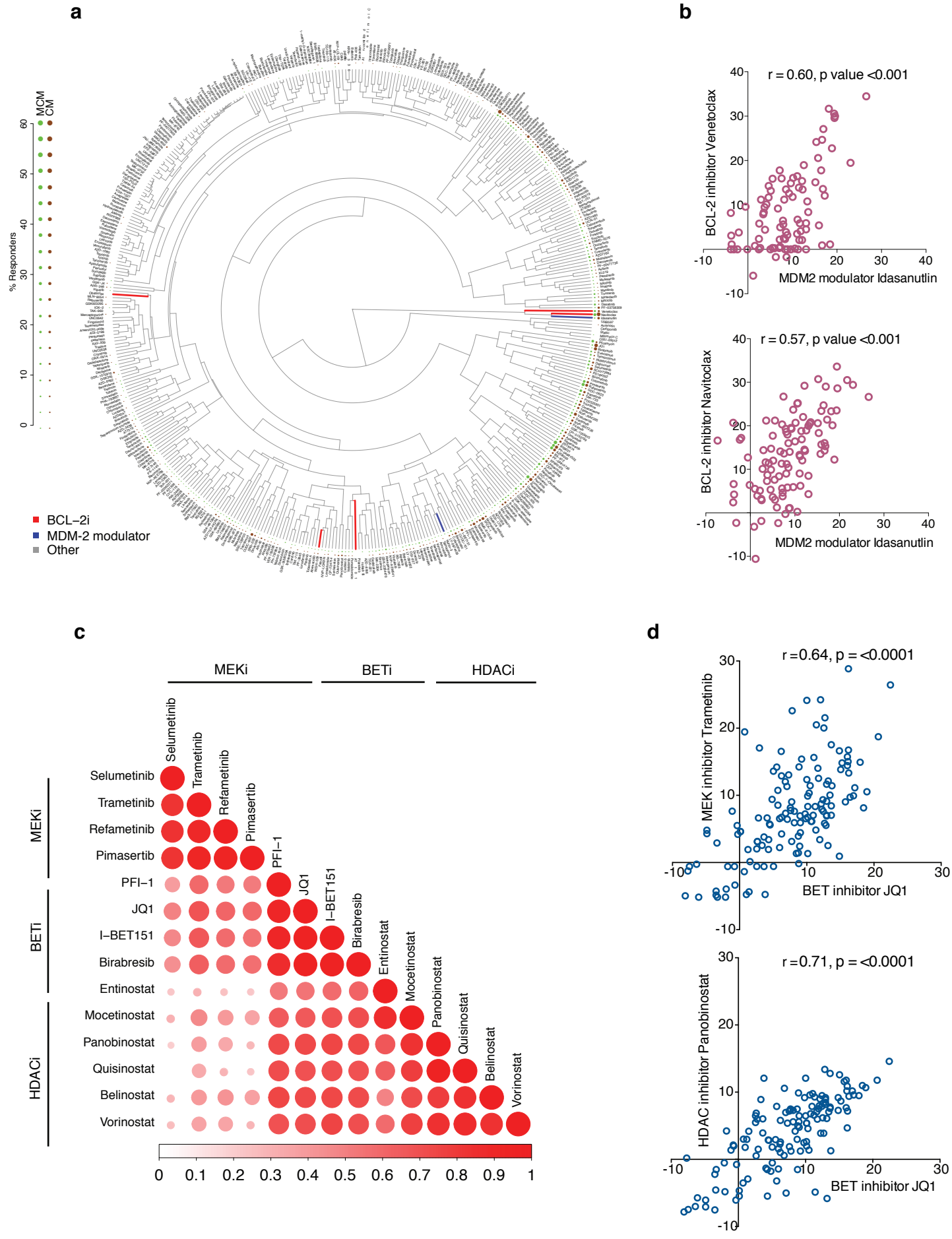

Supplementary Figure 8. Correlation of drug responses. a, Hierarchical clustering of 450 drugs using Euclidian distance and complete linkage indicating a separate group of drugs including BCL-2i venetoclax and navitoclax and MDM2 modulator idasanutlin. **b,** Correlation between idasanutlin and navitoclax or venetoclax where each data point indicating one patient sample. **c,** Correlation map of HDACi, BETi and MEKi where size and color of dot indicating correlation values. **d,** Correlation between BET inhibitors JQ-1 and MEKi trametinib or HDACi panobinostat where each data point indicating one patient sample.

Supplementary figure 9

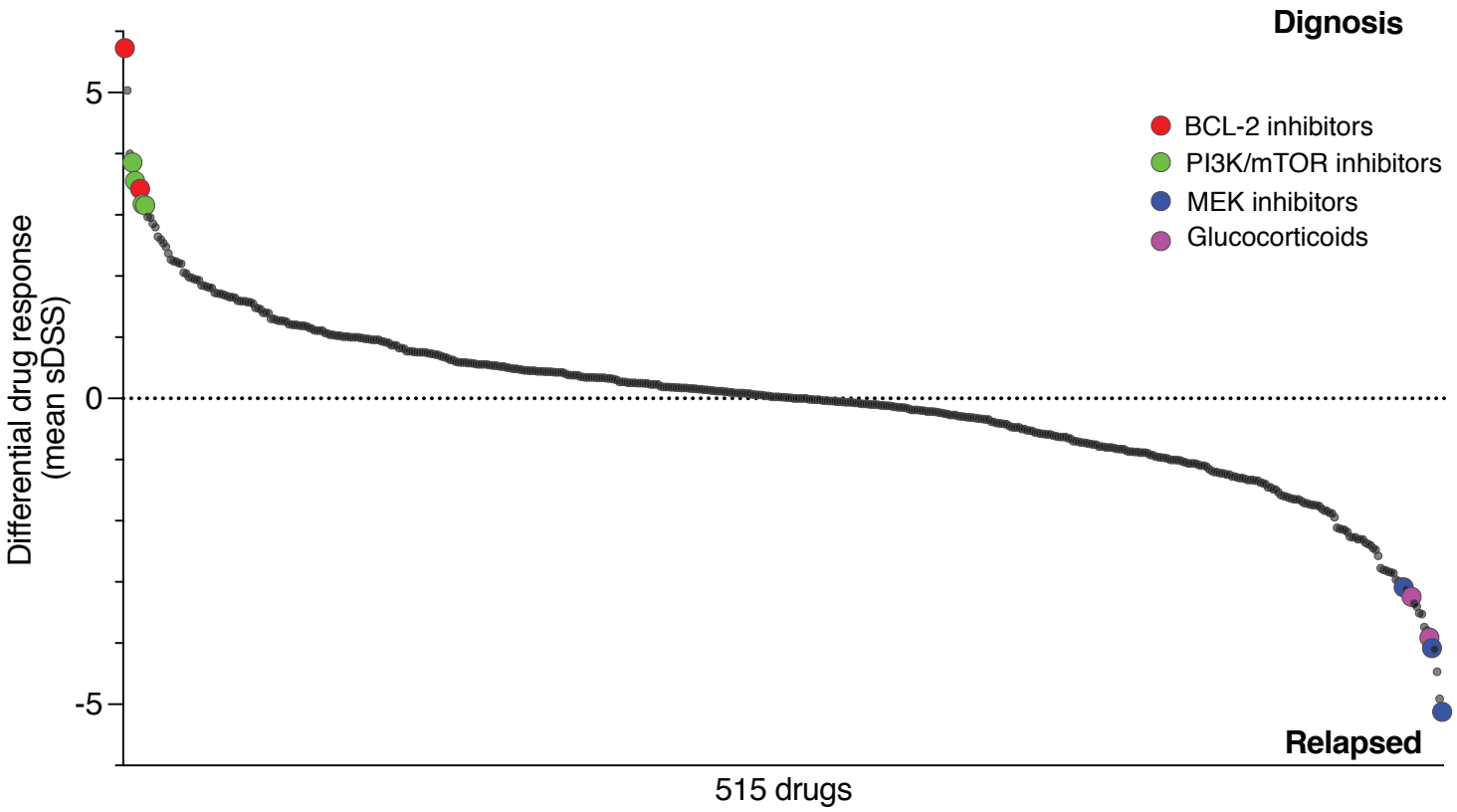

Supplementary Figure 9. Drug response between paired diagnosis and relapsed samples. The plot depicts the mean difference in drug responses (n=515) between diagnosis and relapse samples from the 10 AML patients (AML_001, AML_007, AML_076, AML_078, AML_101, AML_103, AML_112, AML_118, AML_157, AML_084). The highlighted drug class showed top sensitivity in respective diagnosis and relapsed AML samples.

Supplementary figure 10

a

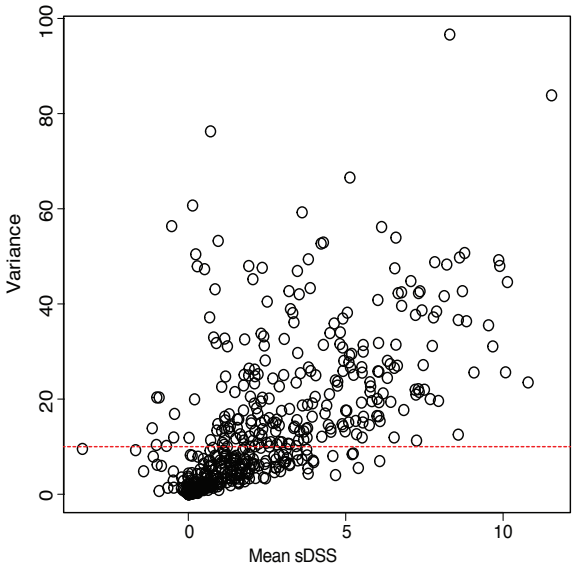

b

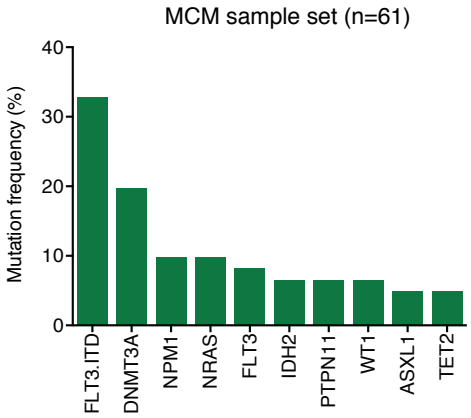

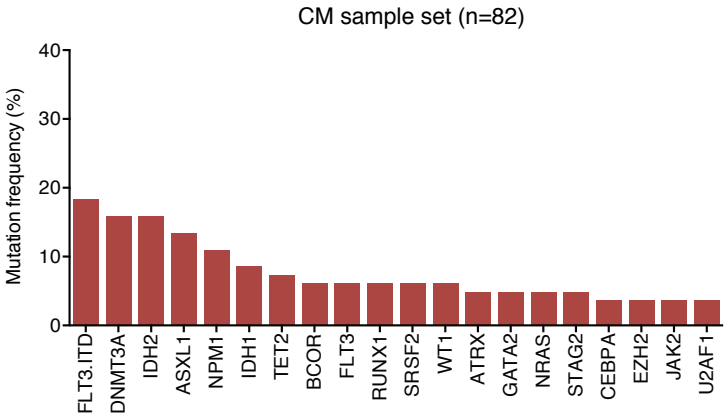

Supplementary Figure 10. Molecular subset specific drug responses. a, Mean sDSS was plotted against variance for 515 chemical compounds to select drugs for further analysis. **b,** Distribution of frequency for key AML related mutations in CM and MCM sample sets.

Supplementary figure 11

a

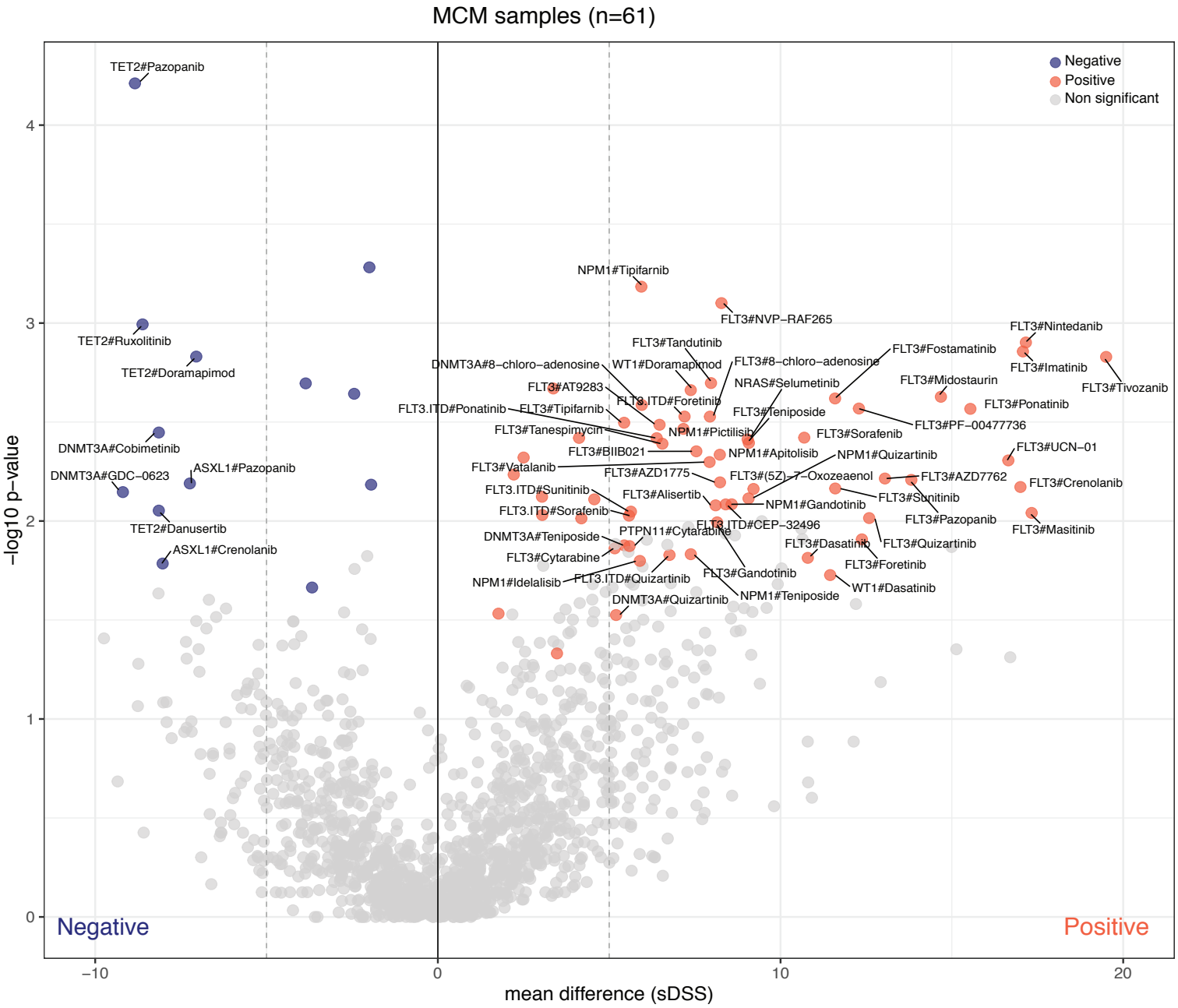

b

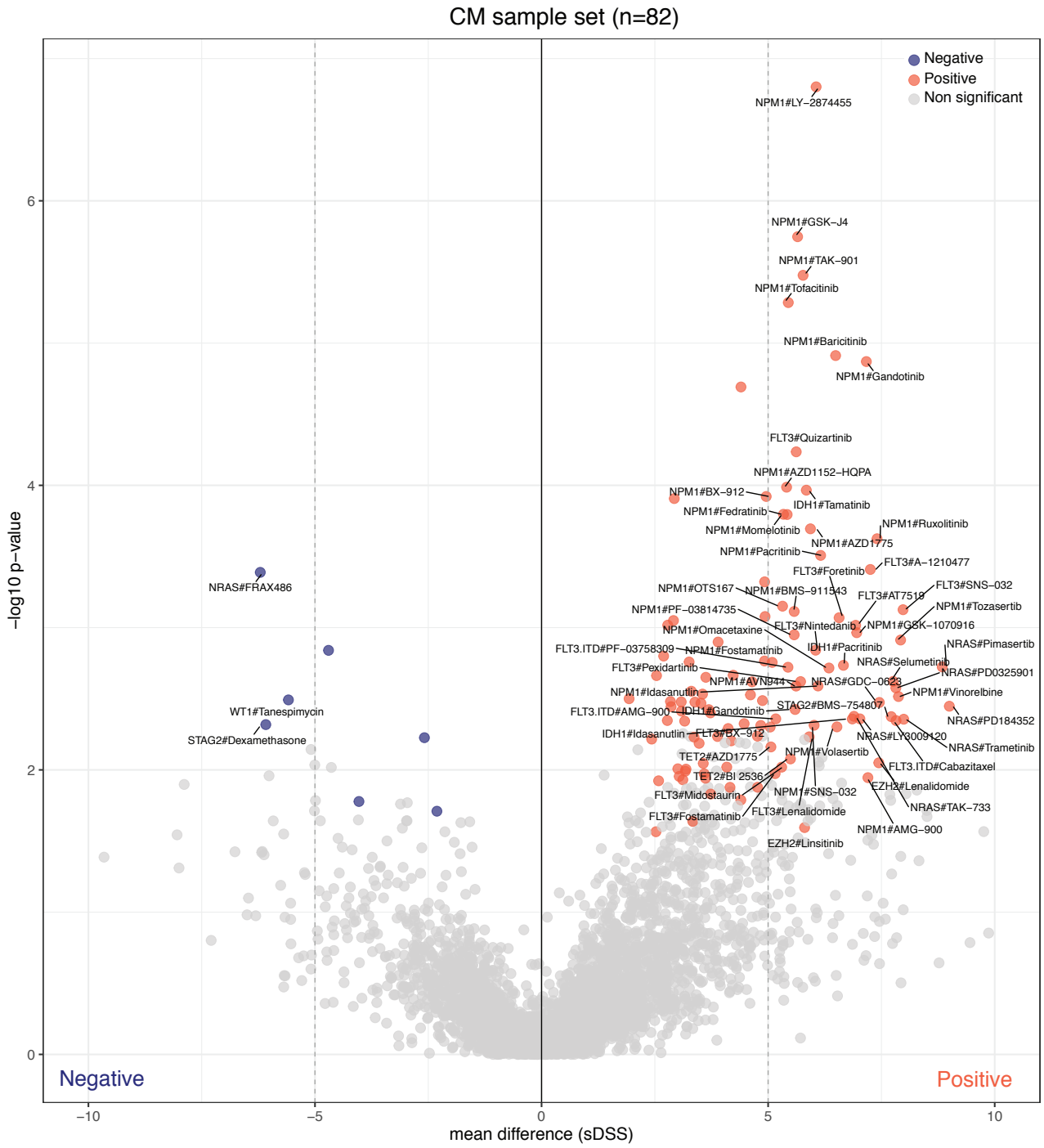
CM sample set (n=82)
Negative
Positive
Non significant
−log10 p−value
mean difference (sDSS)
Negative
Positive
NPM1#LY−2874455
NPM1#GSK−J4
NPM1#TAK−901
NPM1#Tofacitinib
NPM1#Baricitinib
NPM1#Gandotinib
FLT3#Quizartinib
NPM1#AZD1152−HQPA
NPM1#BX−912
IDH1#Tamatinib
NPM1#Fedratinib
NPM1#Momelotinib
NPM1#Ruxolitinib
NPM1#AZD1775
NPM1#Pacritinib
FLT3#A−1210477
FLT3#Foretinib
NRAS#FRAX486
NPM1#OTS167
NPM1#BMS−911543
FLT3#SNS−032
FLT3#AT7519
NPM1#PF−03814735
NPM1#Tozasertib
NPM1#Omacetaxine
FLT3#Nintedanib
NPM1#GSK−1070916
FLT3.ITD#PF−03758309
NPM1#Fostamatinib
IDH1#Pacritinib
NRAS#Pimasertib
FLT3#Pexidartinib
NRAS#Selumetinib
NPM1#AVN944
NRAS#GDC−0623
NRAS#PD0325901
NPM1#Idasanutlin
NPM1#Vinorelbine
WT1#Tanespimycin
STAG2#Dexamethasone
FLT3.ITD#AMG−900
IDH1#Gandotinib
STAG2#BMS−754807
NRAS#PD184352
IDH1#Idasanutlin
FLT3#BX−912
NRAS#LY3009120
NRAS#Trametinib
TET2#AZD1775
NPM1#Volasertib
FLT3.ITD#Cabazitaxel
TET2#BI 2536
EZH2#Lenalidomide
FLT3#Midostaurin
NPM1#SNS−032
NRAS#TAK−733
FLT3#Fostamatinib
FLT3#Lenalidomide
NPM1#AMG−900
EZH2#Linsitinib
6
4
2
0
−10
−5
0
5
10

c

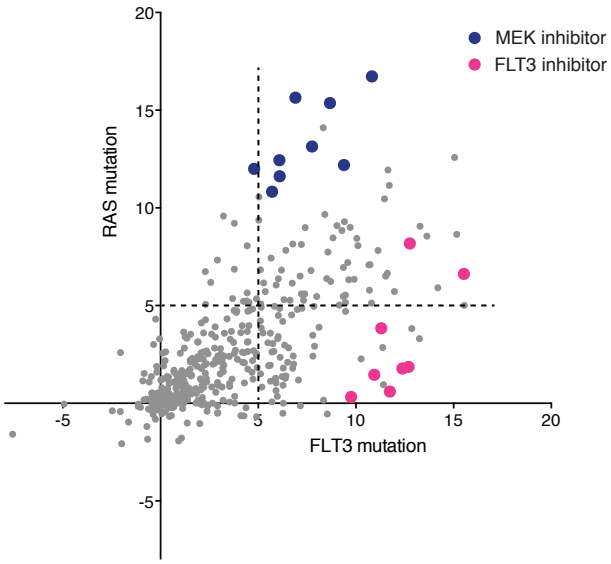
MEK inhibitor
FLT3 inhibitor
RAS mutation
FLT3 mutation
20
15
10
5
-5
5
10
15
20
-5

Supplementary Figure 11. Association analysis of somatic mutations and drug responses. Significant mutated gene-drug pairs in **a,** MCM and **b,** CM sample sets. Sensitive and resistant association indicating the mutation leads to increased or decreased efficacy of drugs compared to wild type samples. **c,** Correlation of average sDSS values between samples carrying FLT3 (ITD and point mutations) mutations and RAS (KRAS and NRAS) depicting FLT3i and MEKi.

Supplementary figure 12

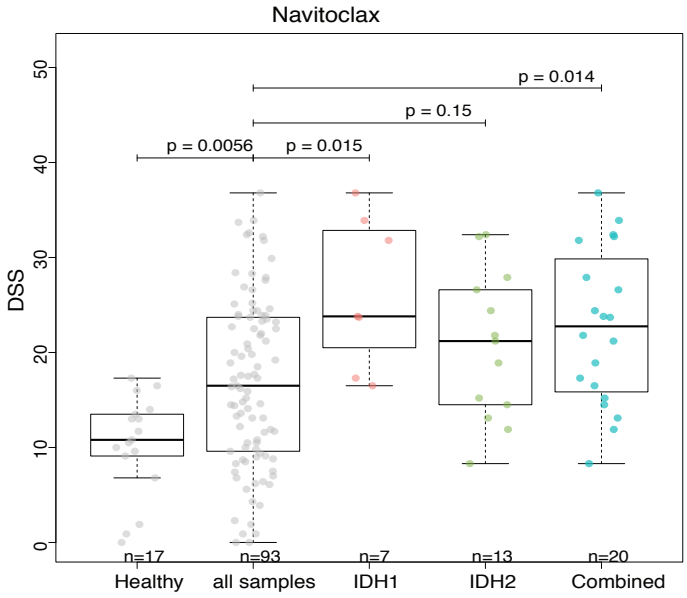

Supplementary Figure 12. Combinations of mutations predicting drug responses. Combination of mutations exist in different samples selected by the LOBICO model to predict efficacy. Navitoclax shows significant association with combination of IDH1 and IDH2 mutations in CM sample set.

Supplementary figure 13

a

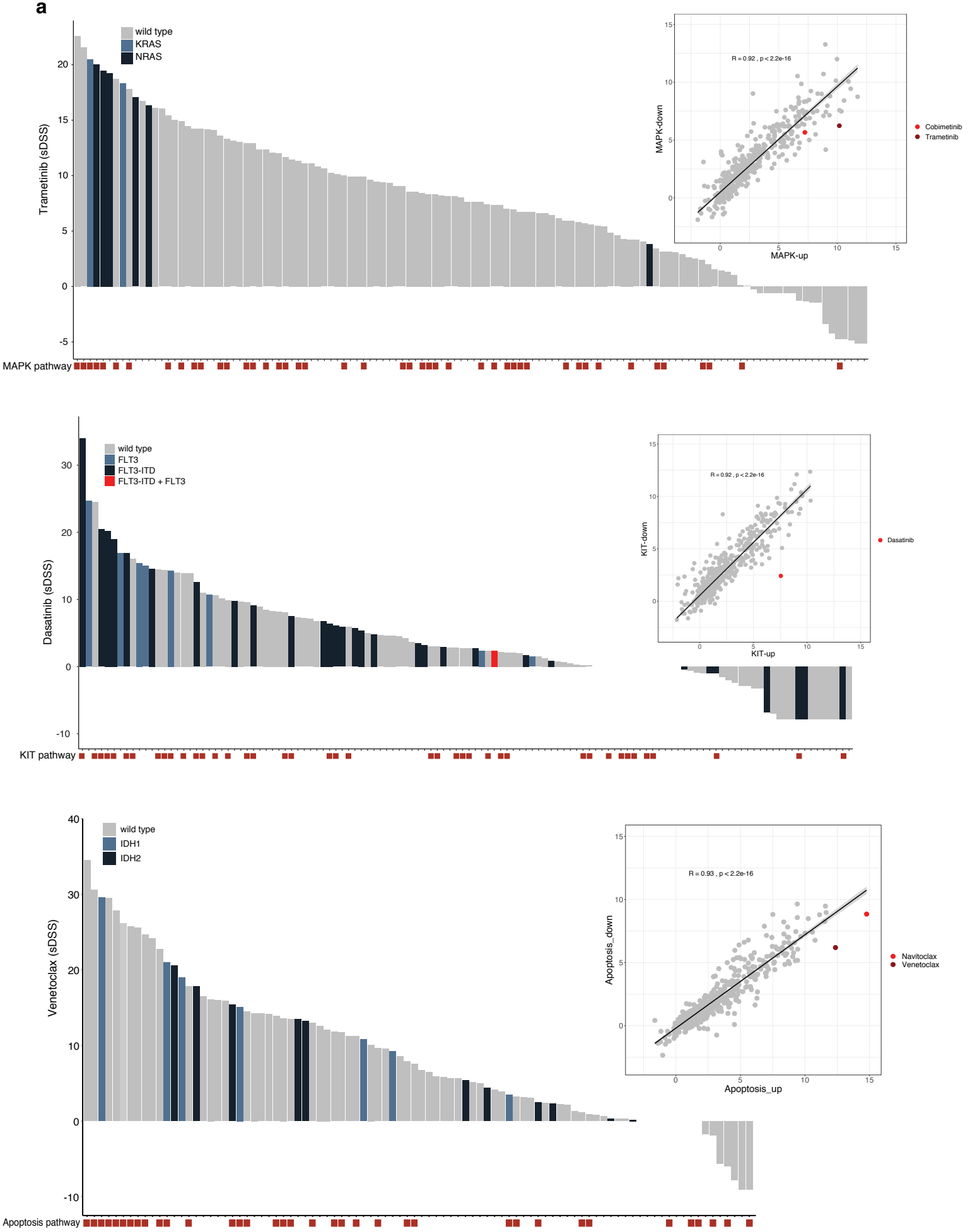

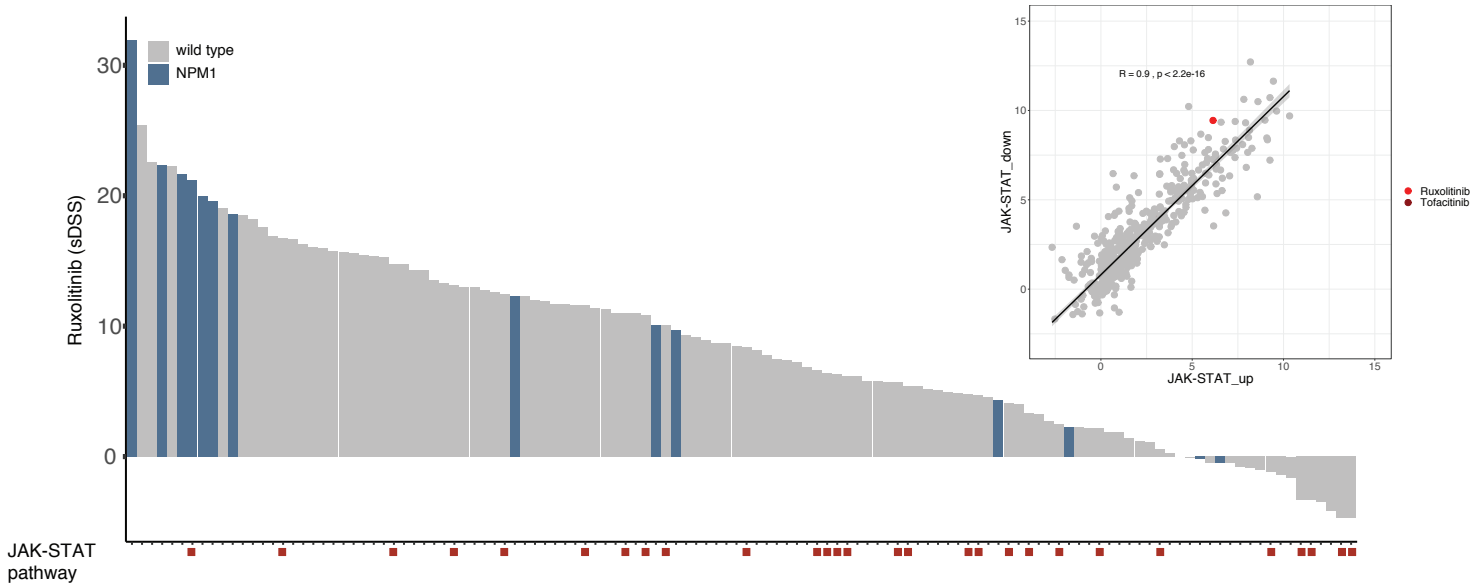
wild type
NPM1
Ruxolitinib (sDSS)
JAK-STAT pathway
R = 0.9 , p < 2.2e-16
JAK-STAT_down
JAK-STAT_up
Ruxolitinib
Tofacitinib

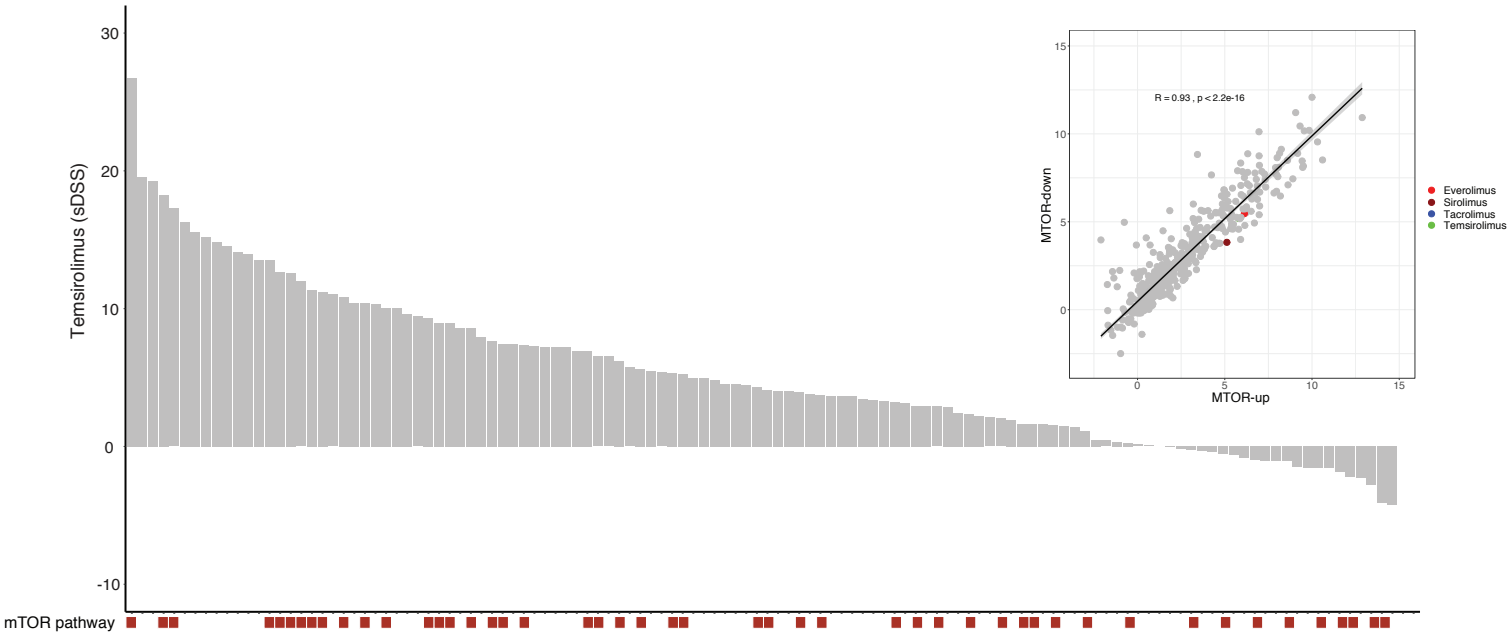
Temsirolimus (sDSS)
mTOR pathway
R = 0.93 , p < 2.2e-16
MTOR-down
MTOR-up
Everolimus
Sirolimus
Tacrolimus
Temsirolimus

b

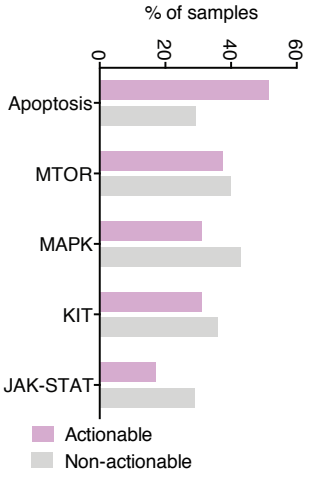
% of samples
Apoptosis
MTOR
MAPK
KIT
JAK-STAT
Actionable
Non-actionable

c

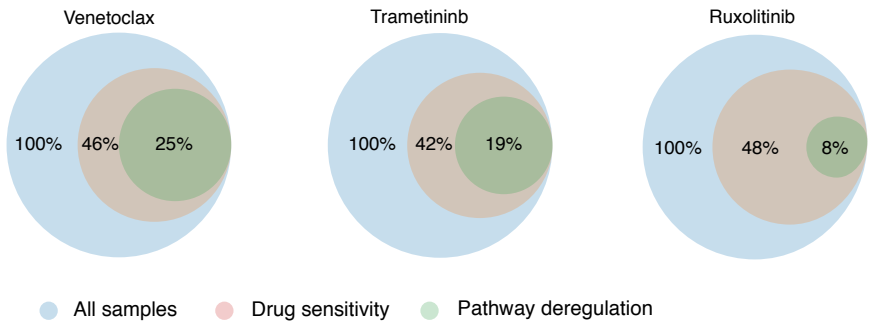
Venetoclax
100%
46%
25%
Trametininb
100%
42%
19%
Ruxolitinib
100%
48%
8%
All samples
Drug sensitivity
Pathway deregulation

Supplementary Figure 13. Pathway activation in individualized drug recommendations. **a,** Response to common effective targeted drugs representing the most effective targeted drug sub-class (trametinib, dasatinib, venetoclax, ruxolitinib, temsirolimus) with respective mutation annotation. The pathway activation was associated with the respective pathway selected based on prior knowledge. Correlation of sDSS between samples with pathway activation and remaining samples illustrated strong sensitivity to the respective drug with pathway activation. **b,** Pathway activation for respective targeted drugs in the percentage of total 122 samples. **c,** Pathway activation coherent with drug efficacy (sDSS>8.7) in total samples.

Supplementary figure 14

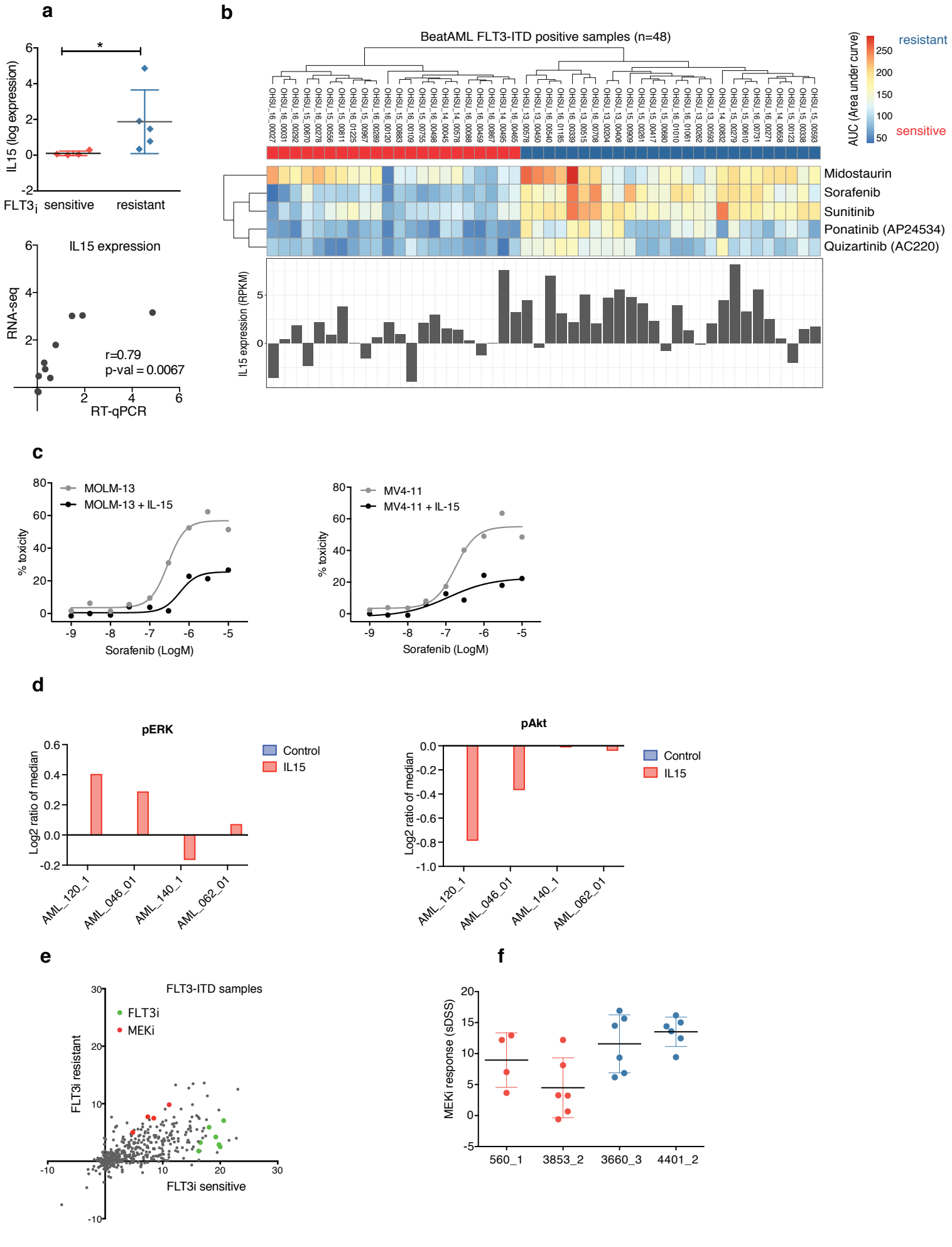

Supplementary Figure 14. Overexpression of IL15 and associated FLT3i resistance. a, RT-qPCR of IL15 gene in FLT3-ITD mutated AML patient samples. Correlation of IL15 gene expression values between RNA-seq (log2 CPM) and RT-qPCR (log2 relative expression). **b,** Hierarchical clustering of 48 FLT3-ITD mutated samples from the BeatAML (Tyner et al. *Nature* 2018(1)) dataset and response to FLT3i/TKi. The expression data of the IL15 gene was taken from the Beat AML dataset and aligned with the heatmap sample order. **c,** Dose-response curves for sorafenib in AML cell lines MOLM-13 and MV4-11 in IL15 stimulated and control cells. **d.** Quantitative analysis of pERK and pAK phosphorylation levels in control and IL15 stimulated FLT3 inhibitor sensitive and resistant AML patient samples. **e,** Correlation of FLT3 and MEK inhibitor responses (sDSS) between FLT3i sensitive (n=5) and resistant (n=8) samples. **f,** MEKi response in FLT3i sensitive (AML_120_01 and AML_046_01) and FLT3i resistant (AML_062_01 and AML_140_01) samples used for phospho-flow cytometry analysis.

Supplementary figure 15

a

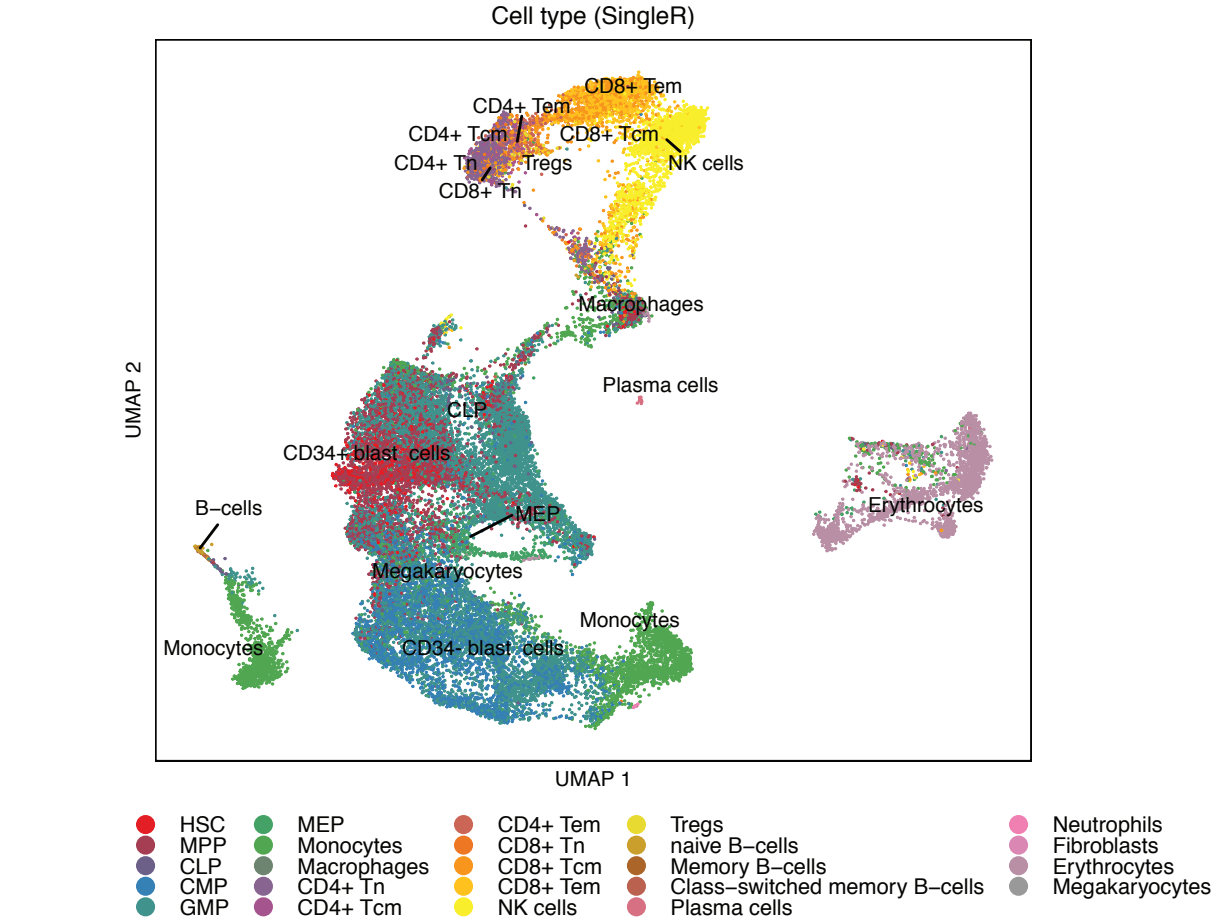

b

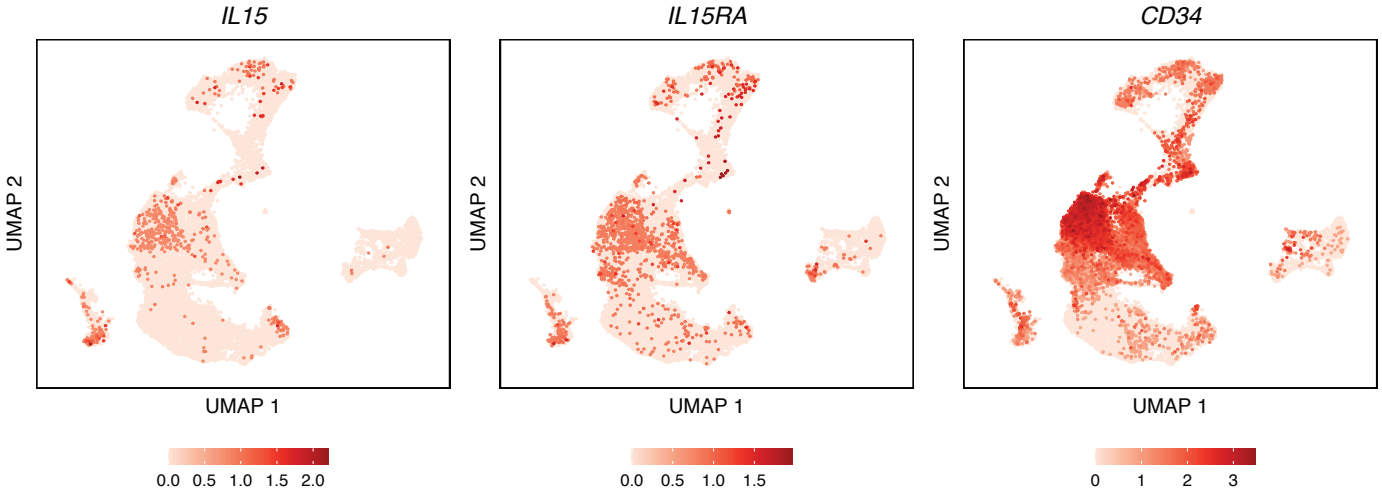

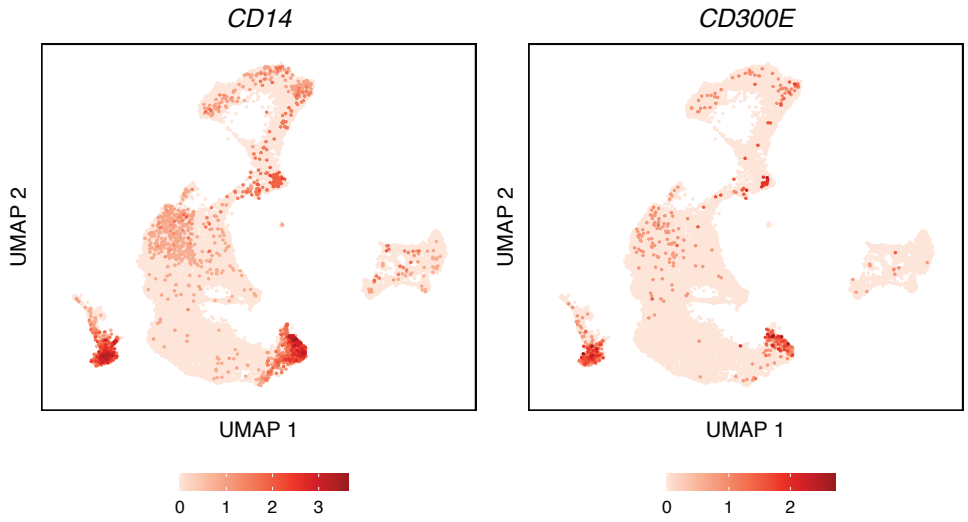
CD14
CD300E
UMAP 2
UMAP 1
0 1 2 3
0 1 2

c

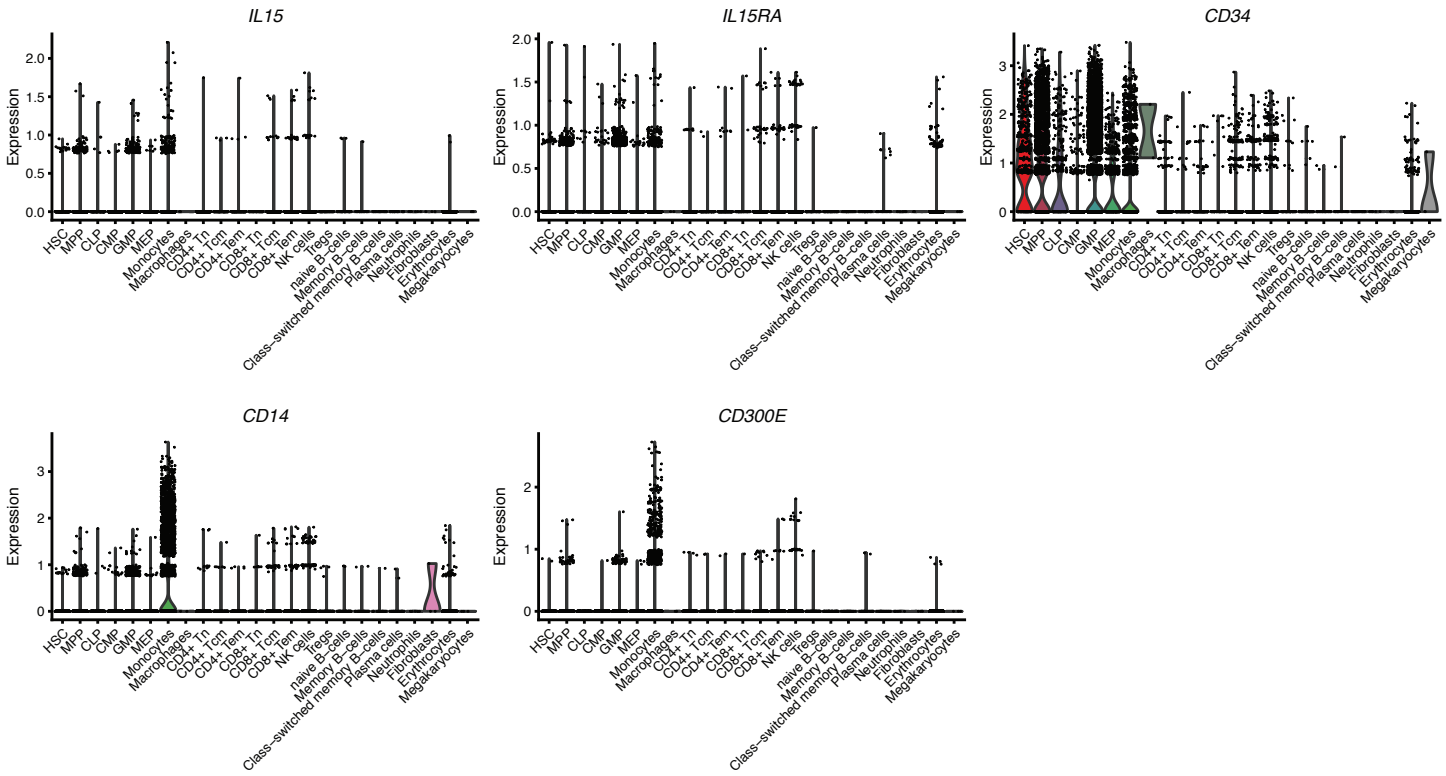
IL15
IL15RA
CD34
CD14
CD300E
Expression
HSC
MPP
CLP
CMP
GMP
MEP
Monocytes
Macrophages
CD4+ Tn
CD4+ Tcm
CD4+ Tem
CD8+ Tn
CD8+ Tcm
CD8+ Tem
NK cells
Tregs
naive B-cells
Memory B-cells
Class-switched memory B-cells
Plasma cells
Neutrophils
Fibroblasts
Erythrocytes
Megakaryocytes

Supplementary Figure 15. Cell type-specific expression of IL15 from single-cell RNA-sequencing data. a, The UMAP plot depicts different cell types from single-cell RNA-seq data of eight different AML patient samples in a published study (Dufva. et al. *Cancer Cell* 2020) The cell types are classified using the reference-based method SingleR. **b,** The UMAP plots demonstrate expression of IL15, IL15 receptor (IL15RA), CD34, CD14 (a marker for monocytes) and CD300E (a marker for monocytes). **c,** The violin plots show expression of IL15, IL15 receptor (IL15RA), CD34, CD14 (a marker for monocytes) and CD300E (a marker for monocytes) stratified by cell type.